Available online at www.sciencedirect.com
SCIENCE DIRECT®
ELSEVIER
Journal of Non-Crystalline Solids 315 (2003) 206–210
JOURNAL OF NON-CRYSTALLINE SOLIDS
www.elsevier.com/locate/jnoncrysol

Letter to the Editor

Glass forming properties of Zr-based bulk metallic alloys

Y. Zhang [a,b,*], D.Q. Zhao [a], M.X. Pan [a], W.H. Wang [a]

[a] Institute of Physics, Chinese Academy of Sciences, Beijing 100080, People's Republic of China
[b] AMM&NS, Singapore-MIT Alliance, National University of Singapore, Singapore 117576, Singapore

Received 17 May 2001; received in revised form 29 July 2002

Abstract

The compositions of $Zr_{41}Ti_{14}Cu_{12}Ni_{10}Be_{23}$ and $Zr_{55}Ni_{10}Cu_{20}Al_{15}$ bulk metallic glasses, were modified by the addition of other elements, such as Nb, Fe, Mg, Y, Ta, and C. The modified alloys also exhibit excellent glass forming ability. The glass transition temperature (T_g), crystallization temperature (T_x), and offset melting temperature (T_l) of the composition modified Zr-based alloys were determined by differential temperature analysis. The results show that the T_g, T_x, and T_l are all sensitive to the composition. The undercooled temperature from T_l to $T_x, \Delta T_l$ defined by $\Delta T_l = T_l - T_x$, has a stronger correlation with the reduced glass transition temperature T_{rg} ($T_{rg} = T_g/T_l$) than that of ΔT_x ($\Delta T_x = T_x - T_g$).

PACS: 61.43.Dq; 65.50.+m; 81.05.Kf; 62.20.Dc

Recently, multicomponent bulk metallic glasses (BMGs) have attracted increasing attention because of their fundamental interests and engineering applications. Many kinds of BMGs have been found; among them, $Pd_{40}Ni_{10}Cu_{30}P_{20}$ and $Zr_{41}Ti_{14}Cu_{12}Ni_{10}Be_{23}$ alloys are two of the best BMG forming alloys [1,2]. To obtain a BMG, observable crystallization in the undercooled melt must be suppressed. Inoue [1] found that the glass forming ability (GFA) of an alloy defined by the critical cooling rate R_c, which is the minimum cooling rate to obtain a BMG, can be evaluated by the values of both T'_{rg} and ΔT_x, where T'_{rg} is defined as T_g/T_m, and ΔT_x is defined as $\Delta T_x = T_x - T_g$, T_g is the glass transition temperature, T_x is the onset crystallization temperature, and T_m is the onset melting temperature. Li [3] showed recently that the best BMG forming alloys are at or near-eutectic compositions, and the reduced glass transition temperature T_{rg} given by T_g/T_l has the highest value at the eutectic composition, where T_l is the offset melting temperature, and this has been confirmed in many alloy systems [3,4].

A great many reports [5–15] show that the GFAs of the alloys, are sensitive to the composition. For example, addition of Cu in PdNiP alloy

* Corresponding author. Address. Department of Materials Science, Faculty of Science, Block S1A02-10, National University of Singapore, 10 Science Drive 4, Lower Kent Ridge Road, Singapore 117543, Singapore. Tel.: +65-68 748 781; fax: +65-67 752 920.

E-mail address: smazy@nus.edu.sg (Y. Zhang).

0022-3093/03/$ - see front matter
PII: S0022-3093(02)01876-8

[16] and Be in Zr-based alloy [2] greatly improve the GFA of the alloys. Generally, R_c is more difficult to measure than T_g, T_x, T_m and T_l. Therefore, the relations between the GFA and the thermal parameters are especially important. Authors have studied this [17]. However, the self-consistency of the parameters has not been studied. In this report, we added some other elements, such as Nb, Ta, Fe, Mg, Y, and C in $Zr_{41}Ti_{14}Cu_{12}Ni_{10}Be_{23}$ and $Zr_{55}Ni_{10}Cu_{20}Al_{15}$ BMG forming alloys. The T_g, T_x, and T_l were measured by DTA. The relationship between ΔT_l ($\Delta T_l = T_l - T_x$) or ΔT_x and T_{rg} was studied.

Ingots of the alloys were prepared by arc melting the mixture of constituent elements in argon atmosphere; the compositions of the alloys are listed in Table 1. As Mg is a volatile element at higher temperature, excessive weight should be added before arc melting. The purities of Zr crystal bar and other constituents are higher than 99.9 wt%. Compositions of the ingots were verified by chemical analysis. The ingots were remelted in a vacuum-sealed quartz tube and quenched in water. As some alloys, such as $Zr_{54}Al_{15}Ni_{10}Cu_{19}Y_2$, $Zr_{53}Al_{14}Ni_{10}Cu_{19}Y_4$, $Zr_{48}Nb_2Cu_{14}Ni_{12}Be_{24}$, and $Zr_{48}Ta_2Cu_{41}Ni_{12}Be_{24}$ alloys, are difficult to form fully amorphous by water quenching method, copper mould injection casting was used [15]. The sample rods with diameter of 3–8 mm were cut into 10 mm-long cylinders and 0.5 mm-thick slices. The cylinders were used for the ultrasonic measurements, and the slices were used for X-ray diffraction (XRD) analysis, differential temperature analysis (DTA) and hardness measurement. XRD was performed by Siemens D5000 X-ray diffractometry with CuK_α radiation. DTA was carried out by Perkin Elmer DTA-7 with a heating rate of 20 K/min, the sample weight about 15 mg was covered by γ-Al_2O_3 powders in an Al_2O_3 crucible purged by argon flow. The density was measured by Archimedian method. The Vickers hardness (H_V) was measured by micro-hardness-71 at a load of 200 g. The acoustic velocities were measured by using a pulse echo overlap method. The travel time of the ultrasonic waves propagating through the sample was measured with a sensitivity of 0.5 ns. The carrier frequency was 10 MHz.

The compositions, and the glass forming properties (T_g, T_x, T_l, T_{rg}, ΔT_x, and ΔT_l) of Zr-based bulk glass forming alloys were listed in Table 1. All the alloys studied have a high T_{rg} (0.61–0.68), indicating the modified Zr-based alloys have excellent GFA [4].

Fig. 1 shows the DTA curves of carbon and Mg + Y additional modified $Zr_{41}Ti_{14}Cu_{12}Ni_{10}Be_{23}$ BMGs. The DTA curve of the $Zr_{41}Ti_{14}Cu_{12}Ni_{10}$-$Be_{23}$ BMG (Fig. 1(a)) shows a glass transition before the crystallization exothermic peaks, and

Table 1
Thermal properties of the Zr-based BMGs with a heating rate of 20 K/min

Properties	T_g (K)	T_x (K)	T_l (K)	ΔT_x (K)	ΔT_l (K)	T_{rg}	Diameters of BMG rods (mm)
$Zr_{41}Ti_{14}Cu_{12.5}Ni_{10}Be_{22.5}$	645	706	1003	61	297	0.64	>10
$Zr_{41}Ti_{14}Cu_{12.5}Ni_8Be_{22.5}C_2$	628	683	997	55	314	0.63	5
$Zr_{41}Ti_{14}Cu_{12.5}Ni_2Be_{22.5}C_8$	629	727	992	98	265	0.63	3
$Zr_{34}Ti_{15}Cu_{10}Ni_{11}Be_{28}Y_2$	650	695	984	45	289	0.66	>8
$[Zr_{41}Ti_{14}Cu_{12.5}Ni_{10}Be_{22.5}]_{98}Y_2$	663	733	1004	70	271	0.66	>8
$Zr_{26}Ti_{10}Cu_8Ni_8Be_{20}Y_4Mg_{24}$	650	700	951	50	251	0.68	5
$Zr_{40}Ti_{15}Cu_{11}Ni_{11}Be_{21.5}Y_1Mg_{0.5}$	630	674	975	44	301	0.65	5
$Zr_{48}Nb_8Cu_{14}Ni_{12}Be_{18}$	656	724	1072	68	348	0.61	8
$Zr_{48}Nb_8Cu_{12}Fe_8Be_{24}$	658	751	1071	93	320	0.61	8
$Zr_{48}Nb_2Cu_{14}Ni_{12}Be_{24}$	668	724	>1062	56	338	0.62	3
$Zr_{48}Ta_2Cu_{14}Ni_{12}Be_{24}$	658	726	>1075	68	349	0.61	3
$Zr_{36}Nb_{12}Cu_{10}Ni_8Be_{20}Y_2Mg_{12}$	653	733	1029	80	296	0.63	5
$Zr_{36}Nb_{12}Cu_{10}Ni_6Fe_2Be_{20}Y_2Mg_{12}$	670	712	1029	42	317	0.65	5
$Zr_{54}Al_{15}Ni_{10}Cu_{19}Y_2$	714	787	1112	73	325	0.64	5
$Zr_{53}Al_{14}Ni_{10}Cu_{19}Y_4$	668	766	1069	98	303	0.62	5

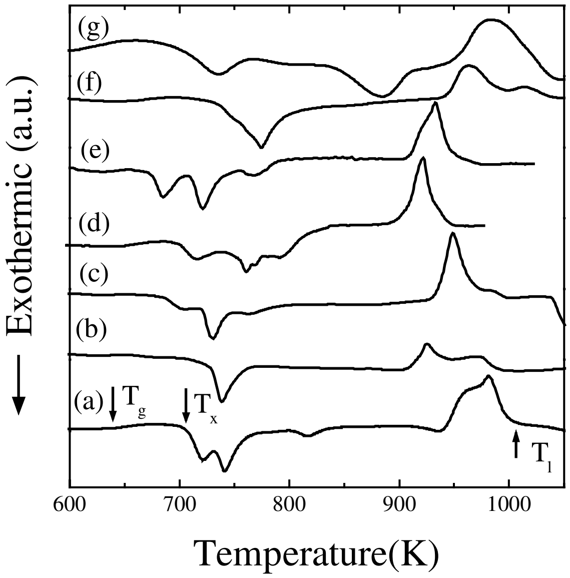

Fig. 1. DTA curves of the Zr/Ti-based BMGs with a heating rate of 20 K/min. (a) $Zr_{41}Ti_{14}$ $Cu_{12}Ni_{10}Be_{23}$, (b) $Zr_{41}Ti_{14}Cu_{12}$-$Ni_{2}Be_{23}C_{8}$, (c) $Zr_{41}Ti_{14}Cu_{12}Ni_{8}Be_{23}C_{2}$, (d) $Zr_{26}Ti_{10}Cu_{8}$ $Ni_{8}Be_{20}$-$Mg_{24}Y_{4}$, (e) $Zr_{40}Ti_{15}Cu_{11}Ni_{11}Be_{21.5}Y_{1}Mg_{0.5}$, (f) $Zr_{33}Ti_{11}Cu_{10}$-$Ni_{8}Be_{18}Mg_{18}Y_{2}$, (g) $[Zr_{41}Ti_{14}Cu_{12}Ni_{10}Be_{23}]_{64}Mg_{36}$.

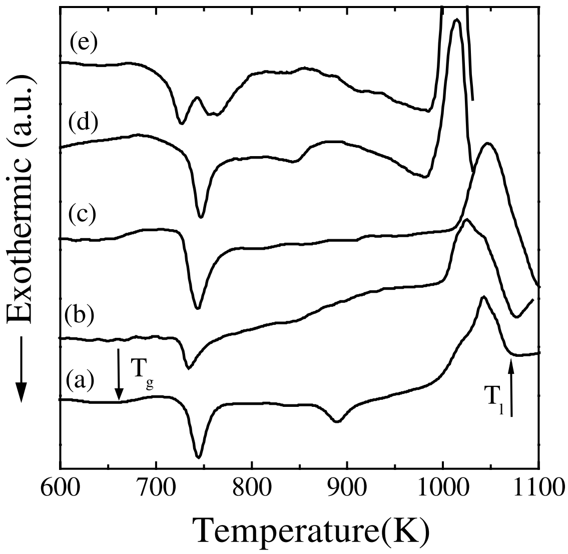

Fig. 2. DTA curves of the Zr-based BMG with a heating rate of 20 K/min. (a) $Zr_{48}Nb_{8}Cu_{14}Ni_{12}Be_{18}$, (b) $Zr_{48}Nb_{2}Cu_{14}Ni_{12}Be_{24}$, (c) $Zr_{48}Ta_{2}Cu_{14}Ni_{12}Be_{24}$, (d) $Zr_{36}Nb_{12}Cu_{10}Ni_{6}Be_{20}Fe_{2}Mg_{12}Y_{2}$, (e) $Zr_{36}Nb_{12}Cu_{10}Ni_{8}Be_{20}Mg_{12}Y_{2}$.

followed by a large endothermic peak corresponding to the melting process [18]. When a small amount of carbon was added to the $Zr_{41}Ti_{14}$-$Cu_{12}Ni_{10}Be_{23}$ alloy, the T_g decreases, the crystallization peak varies significantly and the T_l decreases slightly (Fig. 1(b) and (c)). For the Mg + Y additional Zr-based BMGs, compared with $Zr_{41}Ti_{14}$-$Cu_{12}Ni_{10}Be_{23}$ BMG, T_l decreases and T_x increases. Fig. 1(d) and (e) shows the DTA curves of $Zr_{33}Ti_{11}Cu_{10}Ni_{8}Be_{18}Mg_{18}Y_{2}$ and $[Zr_{41}Ti_{14}Cu_{12}Ni_{10}$-$Be_{23}]_{64}$ Mg_{36} BMGs respectively, both the crystallization and melting process vary significantly. Therefore, the glass transition, crystallization, and melting are all sensitive to the composition. Similarly, the DTA curves of $Zr_{48}Nb_{8}Cu_{14}Ni_{12}Be_{18}$, $Zr_{48}Nb_{2}Cu_{14}Ni_{12}Be_{24}$, $Zr_{48}Ta_{2}Cu_{14}Ni_{12}Be_{24}$, and Mg + Y additional Zr/Nb-based BMGs were shown in Fig. 2, and the DTA curves of the Zr_{54}-$Al_{15}Ni_{10}Cu_{19}Y_{2}$, $Zr_{48}Nb_{8}Cu_{12}Fe_{8}Be_{24}$, $Zr_{53}Al_{14}$-$Ni_{10}Cu_{19}Y_{4}$, $Zr_{34}Ti_{15}Cu_{10}Ni_{11}Be_{28}Y_{2}$, and $[Zr_{41}$-$Ti_{14}Cu_{12}Ni_{10}Be_{23}]_{98}Y_{2}$ BMGs are shown in Fig. 3.

The mechanical properties of some Zr-based BMGs were investigated by ultrasonic study, Vickers hardness (H_V), and density (ρ) measurements. The elastic constants, Young's modulus (E), shear modulus (G), and mechanical properties can be estimated by the ultrasonic velocities and

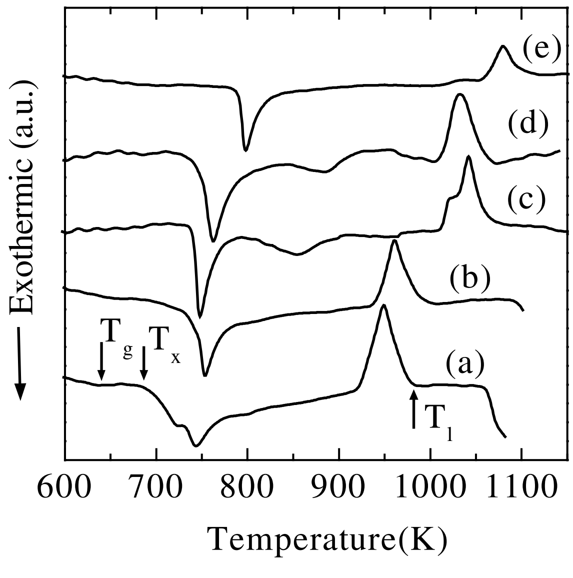

Fig. 3. DTA curves of Zr-based BMGs with a heating rate of 20 K/min. (a) $Zr_{34}Ti_{15}Cu_{10}Ni_{11}Be_{28}Y_{2}$, (b) $[Zr_{41}Ti_{14}Cu_{12}Ni_{10}$-$Be_{23}]_{98}Y_{2}$, (c) Zr_{53} $Al_{14}Ni_{10}Cu_{19}Y_{4}$, (d) $Zr_{48}Nb_{8}Cu_{12}Fe_{8}Be_{24}$, (e) $Zr_{54}Al_{15}Ni_{10}Cu_{19}Y_{2}$.

Table 2
Young's modulus (E), shear modulus (G), density (ρ), and hardness (H_V) of the Zr-based BMGs

Properties	E (GPa)	G (GPa)	ρ (g/cm^3)	H_V (GPa)
$Zr_{41}Ti_{14}Cu_{12.5}Ni_{10}Be_{22.5}$	101.2	37.4	6.13	5.97
$Zr_{48}Nb_8Cu_{14}Ni_{12}Be_{18}$	93.7	34.2	6.70	6.09
$Zr_{48}Nb_8Cu_{12}\ Fe_8Be_{24}$	95.7	35.2	6.44	5.85
$Zr_{53}Al_{14}Ni_{10}Cu_{19}Y_4$	86	31.5	5.93	6.44
$Zr_{54}Al_{15}Ni_{10}Cu_{19}Y_2$	92.1	33.8	6.56	6.49
$Zr_{34}Ti_{15}Cu_{10}Ni_{11}Be_{28}Y_2$	109.8	41.0	5.78	6.07
$Zr_{41}Ti_{14}Cu_{12.5}Ni_8Be_{22.5}C_1$	106	39.5	6.16	6.13
$[Zr_{41}Ti_{14}Cu_{12.5}Ni_{10}Be_{22.5}]_{98}Y_2$	107.6	40.3	5.86	6.76
$Zr_{40}Ti_{15}Cu_{11}Ni_{11}Be_{21.5}Y_1Mg_{0.5}$	94.2	34.7	6.05	5.74

density according to the solid theory [12], the obtained data are summarized in Table 2.

According to the classical crystallization theory of the undercooled melts [19], the temperature-time-transformation diagram shows a 'C' shape curve. R_c is the lowest cooling rate to bypass the nose of the 'C' curve, and R_c can be estimated by the following equation [20]:

$$R_c = \frac{T_l - T_N}{t_N}, \quad (1)$$

where T_N is the crystallization temperature at the nose of the 'C' curve, t_N is incubation time of the nose temperature. T_N is not easy to be measured by DSC, but we can estimate it by using T_x, then $\Delta T_l = T_l - T_x$ is proportional to R_c. Fig. 4 shows the linear fit of ΔT_x with T_{rg} (Fig. 4(a)), and ΔT_l with T_{rg} (Fig. 4(b)), all of the data are obtained from Table 1. The fitting equations are as following:

$$\Delta T_x = 388.45 - 505.84 T_{rg}, \quad r = 0.56, \quad (2)$$

$$\Delta T_l = 958.53 - 1026.62 T_{rg}, \quad r = 0.74. \quad (3)$$

For each equation, r is the correlation coefficient of the fit, when $r = 1$, no error between the fit and the data, the higher the r value, the better the fit. So the fit of ΔT_l with T_{rg} ($r = 0.74$) is better than that of ΔT_x with T_{rg} ($r = 0.56$). This indicates that ΔT_l, like T_{rg}, can be used to evaluate the GFA of an alloy, and the lower the ΔT_l, the better the GFA. However, the dependence of ΔT_x with T_{rg} is relatively weak ($r = 0.56$). If the relation (Eq. (2)) is right, the higher values of ΔT_x corresponding to the lower value of T_{rg}. As ΔT_x is a scale of thermal stability, it means the thermal stability is opposite to the GFA, this is in a good agreement with Ref. [4], and different from that of Ref. [1]. Chen [21] used ΔT_g, defined by $\Delta T_g = T_l - T_g$, to evaluate the GFA of an alloy, the lower the ΔT_g, the better the GFA. In fact, ΔT_g and T_{rg} (from their definition) have the same results to evaluate the GFA of an alloy. Anyway, ΔT_g can be denoted as

$$\Delta T_g = \Delta T_l + \Delta T_x. \quad (4)$$

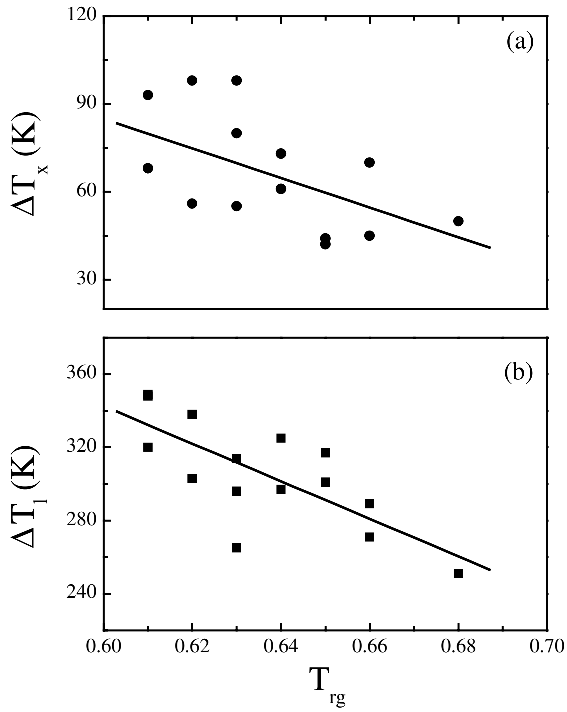

Fig. 4. ΔT_x and ΔT_l as a function of T_{rg} for the data collected from Table 1. (a) ΔT_x versus T_{rg}, (b) ΔT_l versus T_{rg}.

As ΔT_l has a strong correlation with T_{rg}, it is the dominant part of T_g. However, the higher value of ΔT_x may increase the ΔT_g, and decrease the T_{rg}. Therefore, if T_{rg} is a scale of GFA, and ΔT_x is a scale of thermal stability, they may be opposite.

The compositions of $Zr_{41}Ti_{14}Cu_{12}Ni_{10}Be_{23}$ and $Zr_{55}Ni_{10}Cu_{20}Al_{15}$ BMGs were modified by element additional methods. The glass transition, crystallization, and melting are all sensitive to the composition. The ΔT_l as well as T_{rg} (or ΔT_g), can be a scale for the GFA of an alloy. While ΔT_x, is opposite to T_{rg}, which indicates that the excellent thermal stability may deteriorate the GFA in the Zr-based BMGs.

Acknowledgements

Y.Z. would like to thank the helpful discussion with Professor B. Yao, and also thanks to the support from Singapore–MIT Alliance.

References

[1] A. Inoue, Acta Mater. 48 (2000) 279.
[2] A. Peker, W.L. Johnson, Appl. Phys. Lett. 63 (1993) 2342.
[3] Z.P. Lu, H. Tan, Y. Li, S.C. Ng, Scr. Mater. 42 (2000) 667.
[4] T.A. Waniuk, I. Schroers, W.L. Johnson, Appl. Phys. Lett. 78 (9) (2001) 1213.
[5] C.C. Hays, C.P. Kim, W.L. Johnson, Phys. Rev. Lett. 84 (13) (2000) 2901.
[6] D.V. Louzguine, A. Inoue, J. Mater. Res. 14 (11) (1999) 4426.
[7] C.F. Li, J. Saida, M. Matsushida, A. Inoue, Scr. Mater. 42 (2000) 923.
[8] W. Liu, W.L. Johnson, J. Mater. Res. 11 (1996) 2388.
[9] H.G. Kang, E.S. Park, W.T. Kim, D.H. Kim, H.K. Cho, Mater. Trans., JIM 41 (7) (2000) 846.
[10] H. Choi-Yim, R. Busch, W.L. Johnson, J. Appl. Phys. 83 (12) (1998) 7993.
[11] X. Rao, P.C. Si, W.H. Wang, Y. Zhang, Z. Xu, J.N. Wang, J. Mater. Sci. Lett. 19 (2000) 1499.
[12] W.H. Wang, Q. Wei, H. Friedrich, Phys. Rev. B 57 (1998) 8211.
[13] D.Q. Zhao, Y. Zhang, Y.X. Zhuang, M.X. Pan, W.H. Wang, Mater. Trans., JIM 41 (11) (2001) 1427.
[14] Y. Zhang, D.Q. Zhao, R.J. Wang, M.X. Pan, W.H. Wang, Mater. Trans., JIM 41 (11) (2001) 1423.
[15] Y. Zhang, M.X. Pan, D.Q. Zhao, R.J. Wang, W.H. Wang, Mater. Trans., JIM 41 (11) (2001) 1410.
[16] A. Inoue, N. Nishiyama, T. Matsuda, Mater. Trans., JIM 37 (1996) 181.
[17] Y. Li, S.C. Ng, C.K. Ong, H.H. Hng, T.T. Goh, Scr. Mater. 36 (7) (1999) 783.
[18] W.H. Wang, L.L. Li, M.X. Pan, R.J. Wang, Phys. Rev. B 63 (2001) 052204.
[19] D.M. Herlach, Mater. Sci. Eng. R 12 (1994) 177.
[20] N. Nishiyama, A. Inoue, Acta Mater. 47 (5) (1999) 1487.
[21] H.S. Chen, Acta Metall. 22 (1974) 1505.